Atmos. Chem. Phys. Discuss., doi:10.5194/acp-2016-215, 2016
Manuscript under review for journal Atmos. Chem. Phys.
Published: 13 May 2016

Atmospheric Chemistry and Physics Discussions

Ozone Production and Its Sensitivity to NO_x and VOCs: Results from the DISCOVER-AQ Field Experiment, Houston 2013

Gina M. Mazzuca[1], Xinrong Ren[1,2,*], Christopher P. Loughner[2,3,4], Mark Estes[5], James H. Crawford[6], Kenneth E. Pickering[1,4], Andrew J. Weinheimer[7], and Russell R. Dickerson[1]

[1]Department of Atmospheric and Oceanic Science, University of Maryland, College Park, MD 20742, USA

[2]Air Resources Laboratory, National Oceanic and Atmospheric Administration, College Park, MD 20740, USA

[3]Earth System Science Interdisciplinary Center, University of Maryland, College Park, MD 20740, USA

[4]NASA Goddard Space Flight Center, Greenbelt, MD 20771, USA

[5]Texas Commission on Environmental Quality, Austin, TX 78711, USA

[6]NASA Langley Research Center, Hampton, VA 23681, USA

[7] National Center for Atmospheric Research, Boulder, CO 80307, USA

*Correspondence to: X. Ren (ren@umd.edu)

Abstract An observation-constrained box model based on the Carbon Bond mechanism, Version 5 (CB05), was used to study photochemical processes along the NASA P-3B flight track and spirals over eight surface sites during the September 2013 Houston, Texas deployment of the NASA DISCOVER-AQ campaign. Data from this campaign provided an opportunity to examine and improve our understanding of atmospheric photochemical oxidation processes related to the formation of secondary air pollutants such as ozone (O_3). O_3 production and its sensitivity to NO_x and VOCs were calculated at different locations and times of day. Ozone production efficiency (OPE), defined as the ratio of the ozone production rate to the NO_x oxidation rate, was calculated using the observations and the simulation results of the box and Community Multiscale Air Quality (CMAQ) models. Correlations of these results with other parameters, such as radical sources and NO_x mixing ratio, were also evaluated. It was generally found that O_3 production tends to be more VOC sensitive in the morning along with high ozone production rates, suggesting that control of VOCs may be an effective way to control O_3 in Houston. In the

Atmos. Chem. Phys. Discuss., doi:10.5194/acp-2016-215, 2016
Manuscript under review for journal Atmos. Chem. Phys.
Published: 13 May 2016

Atmospheric Chemistry and Physics Discussions

afternoon, O_3 production was found to be mainly NO_x sensitive with some exceptions. O_3 production at near major emissions sources such as Deer Park was mostly VOC sensitive for the entire day, other urban areas near Moody Tower and Channelview were VOC sensitive or in the transition regime, and areas farther from downtown Houston such as Smith Point and Conroe were mostly NO_x sensitive for the entire day. It was also found that the control of NO_x emissions has reduced O_3 concentrations over Houston, but led to larger OPE values. The results from this work strengthen our understanding of O_3 production; they indicate that controlling NO_x emissions will provide air quality benefits over the greater Houston metropolitan area in the long run, but in selected areas controlling VOC emissions will also be beneficial.

Keywords Ozone production; Houston; DISCOVER-AQ

1. Introduction

Understanding the non-linear relationship between ozone production and its precursors is critical for the development of an effective ozone (O_3) control strategy. Despite great efforts undertaken in the past decades to address the problem of high ozone concentrations, our understanding of the key precursors that control tropospheric ozone production remains incomplete and uncertain [Molina and Molina, 2004; Xue et al., 2013]. Atmospheric ozone levels are determined by emissions of ozone precursors, atmospheric photochemistry, and transport [Jacob, 1999; Xue et al., 2013]. A major challenge in regulating ozone pollution lies in comprehending its complex and non-linear chemistry with respect to ozone precursors, i.e., nitrogen oxides (NO_x) and volatile organic compounds (VOCs) that varies with time and location (Figure 1). Understanding of the non-linear relationship between ozone production and its precursors is critical for the development of an effective ozone control strategy.

Sensitivity of ozone production to NO_x and VOCs represents a major uncertainty for oxidant photochemistry in urban areas [Sillman et al., 1995; 2003]. In urban environments, ozone is formed through photochemical processes when its precursors NO_x and VOCs are emitted into the atmosphere from many sources. Depending on physical and chemical conditions, the production of ozone can be either NO_x-sensitive or VOC-sensitive due to the complexity of these photochemical processes. Therefore, effective ozone control strategies rely heavily on the accurate understanding of how ozone responds to reduction of NO_x and VOC emissions, usually

Atmos. Chem. Phys. Discuss., doi:10.5194/acp-2016-215, 2016
Manuscript under review for journal Atmos. Chem. Phys.
Published: 13 May 2016

simulated by photochemical air quality models [e.g., Sillman et al., 2003; Lei et al., 2004; Mallet and Sportisse, 2005; Li et al, 2007; Chen et al., 2010; Tang et al., 2010; Xue et al., 2013; Goldberg et al., 2016]. However, those model-based studies have inputs or parameters subject to large uncertainties that can affect not only the simulated levels of ozone but also the ozone dependence on its precursors.

There are a limited number of observation-based studies on ozone production and its sensitivity to NO_x and VOCs. Using in-situ aircraft observations, Kleinman et al. [2005a] studied five U.S. cities and found that ozone production rates vary from nearly zero to 155 ppb hr^{-1} with differences depending on precursor concentrations NO_x, and VOCs. They also found that in Houston, NO_x and light olefins are co-emitted from petrochemical facilities leading to the highest ozone production of the five cities [Kleinman et al., 2005a]. Using the data collected at a single surface location during the Study of Houston Atmospheric Radical Precursors (SHARP) in spring 2009, the temporal variation of O_3 production was observed: VOC-sensitive in the early morning and NO_x-sensitive for most of the afternoon [Ren et al., 2013]. This is similar to the behavior observed in two previous summertime studies in Houston: the Texas Air Quality Study in 2000 (TexAQS 2000) and the TexAQS II Radical and Aerosol Measurement Project in 2006 (TRAMP 2006) [Mao et al., 2010; Chen et al., 2010]. In a more recent study using measurements in four cities in China, ozone production was found to be in a VOC-sensitive regime in both Shanghai and Guangzhou, but in a mixed regime in Lanzhou [Xue et al., 2013]. More investigations of spatial and temporal variations of ozone production and its sensitivity to NO_x and VOCs are thus needed to provide a scientific basis to develop a non-uniform emission reduction strategy for O_3 pollution control in urban areas like Houston.

During the Deriving Information on Surface Conditions from COlumn and VERtically Resolved Observations Relevant to Air Quality (DISCOVER-AQ) campaign in Houston in September 2013, a comprehensive suite of measurements were collected from various platforms including the National Aeronautics and Space Administration (NASA) P-3B and B-200 aircraft, ground surface sites, and mobile laboratories [DISCOVER-AQ whitepaper]. In-situ measurements on the NASA P-3B directly related to satellite observations of air quality include ozone (O_3), nitrogen dioxide (NO_2), formaldehyde (HCHO), and aerosol optical and microphysical properties. Additional critical variables needed for retrievals and data interpretation were also measured including atmospheric state (temperature, pressure, wind speed

Atmos. Chem. Phys. Discuss., doi:10.5194/acp-2016-215, 2016
Manuscript under review for journal Atmos. Chem. Phys.
Published: 13 May 2016

Atmospheric Chemistry and Physics Discussions

and wind direction), water vapor (H_2O), carbon monoxide (CO), methane (CH_4), carbon dioxide (CO_2), nitric oxide (NO), the other components of reactive nitrogen, and aerosol inorganic and organic composition.

Eight surface monitoring stations were selected where the P-3B conducted vertical spirals (Figure 2). These monitoring stations provided in situ observations of trace gases (O_3, CO, NO, NO_y, SO_2), and at a subset of these stations aerosol lidar observations, NO_2 columns, and balloon soundings of O_3, NO_2, NO_x and water vapor were conducted. The eight surface sites (Smith Point, Galveston, Manvel Croix, Deer Park, Channelview, Conroe, West Houston, and Moody Tower) were chosen for the deployment with regard to the presence or absence of complementary chemical and meteorological measurements; the strength and likely impact of nearby point and mobile emission sources; the topography, height, and extent of nearby structures and vegetation; and any characteristic which might render the site physically or chemically unrepresentative of the surrounding area [DISCOVER-AQ whitepaper].

2. Methods

2.1 Ozone production Scenarios and Sensitivity

During the day, the photochemical O_3 production rate is essentially the production rate of NO_2 molecules from HO_2 + NO and RO_2 + NO reactions [Finlayson-Pitts and Pitts, 2000]. The net instantaneous photochemical O_3 production rate, $P(O_3)$, can be written approximately as the following equation:

$$P(O_3) = k_{HO_2+NO}[HO_2][NO] + \sum k_{RO_{2i}+NO}[RO_{2i}][NO] - k_{OH+NO_2+M}[OH][NO_2][M] - P(RONO_2) \\ -k_{HO_2+O_3}[HO_2][O_3] - k_{OH+O_3}[OH][O_3] - k_{O(^1D)+H_2O}[O(^1D)][H_2O] - L(O_3 + alkenes) \quad (1)$$

where, *k terms* are the reaction rate coefficients; RO_{2i} is the individual organic peroxy radicals. The negative terms in Eq. (1) correspond to the reaction of OH and NO_2 to form nitric acid, the formation of organic nitrates, $P(RONO_2)$, the reactions of OH and HO_2 with O_3, the photolysis of O_3 followed by the reaction of $O(^1D)$ with H_2O, and O_3 reactions with alkenes. Ozone is additionally destroyed by dry deposition.

The dependence of O_3 production on NO_x and VOCs can be categorized into two typical scenarios: NO_x sensitive and VOC sensitive. The method proposed by Kleinman [2005b] was used to evaluate the O_3 production sensitivity using the ratio of L_N/Q, where L_N is the radical loss via the reactions with NO_x and Q is the total primary radical production. Because the radical

Atmos. Chem. Phys. Discuss., doi:10.5194/acp-2016-215, 2016
Manuscript under review for journal Atmos. Chem. Phys.
Published: 13 May 2016

Atmospheric Chemistry and Physics Discussions

production rate is approximately equal to the radical loss rate, this L_N/Q ratio represents the fraction of radical loss due to NO_x. It was found that when L_N/Q is significantly less than 0.5, the atmosphere is in a NO_x-sensitive regime, and when L_N/Q is significantly greater than 0.5, the atmosphere is in a more VOC-sensitive regime [Kleinman et al., 2001; Kleinman, 2005b]. Note that the contribution of organic nitrates impacts the cut-off value for L_N/Q to determine the ozone production sensitivity to NO_x or VOCs and this value may vary slightly around 0.5 in different environments [Kleinman, 2005b].

2.2 Box Model Simulations

An observation-constrained box model with the Carbon Bond Mechanism Version 2005 (CB05) was used to simulate the oxidation processes in Houston during DISCOVER-AQ. Measurements made on the P-3B were used as input to constrain the box model. From the box model results, the ozone production rate and its sensitivity to NO_x and VOCs were calculated allowing us to calculate ozone production efficiency at different locations and at different times of day.

CB05 is a well-known chemical mechanism that has been actively in use in research and regulatory applications [Yarwood et al., 2005]. CB05 is an updated version of CB4. In contrast to the previous version, (1) inorganic reactions are extended to simulate remote to polluted urban conditions; and (2) two extensions are available to be added to the core mechanism for modeling explicit species and reactive chlorine chemistry. Organic species are lumped according to the carbon bond approach, that is, bond type, e.g., carbon single bond and double bond. Reactions are aggregated based on the similarity of carbon bond structure so that fewer surrogate species are needed in the model. Some organics (e.g., organic nitrates and aromatics) are lumped. The original mechanism was used while kinetic data were updated based on the most recent chemical kinetic data evaluations [e.g., Atkinson et al., 2004; 2006; 2007; 2008; Sander et al, 2011]. The lifetime of alkyl nitrates is too long in CB05 and has been corrected in CB6r2 [Canty et al., 2015], but this should have minimal impact on our findings because the model is constrained to observations as indicated below.

The box model was run using measurements, including long-lived inorganic and organic compounds and meteorological parameters (temperature, pressure, humidity, and photolysis frequencies), from the NASA P-3B. One-minute archived data were used as model input

Atmos. Chem. Phys. Discuss., doi:10.5194/acp-2016-215, 2016
Manuscript under review for journal Atmos. Chem. Phys.
Published: 13 May 2016

(available at http://www-air.larc.nasa.gov/missions/discover-aq/discover-aq.html). The model ran for 24 hours for each data point to allow most calculated reactive intermediates to reach steady state, but short enough to prevent the buildup of secondary products. A deposition lifetime of two days was assumed for all calculated species to avoid unexpected accumulation of these species in the model. At the end of 24 hours, the model generated time series of OH, HO_2, RO_2, and other reactive intermediates. The box model covered the entire P-3B flight track during DISCOVER-AQ, including the eight science sites where the P-3B conducted spirals. Note that unlike a three-dimensional chemical transport model, the zero-dimensional box model simulations did not include advection and emissions, although advection and emissions are certainly important factors for the air pollution formation. Because all of the long-lived radical and O_3 precursors were measured and used to constrain the box model calculations, the advection and emissions can be neglected for the calculated radicals and their production and loss rates. The box model analysis is necessary for ozone production and its sensitivity to NO_x and VOCs because the box model was constrained to measured species (e.g., NO, NO_2, CO, HCHO, etc.) and meteorological parameters (e.g., photolysis frequencies) that are essential to calculate ozone production rates. Even though there is good agreement in general between the box model and the 3D model, there are still some differences between the measurements and the output from the 3D model, e.g., NOx, CO, HCHO and photolysis frequencies.

2.3 WRF-CMAQ Model Simulations

The WRF model was run from 18 August 2013 to 1 October 2013 with nested domains with horizontal resolutions of 36, 12, 4, and 1 km and 45 vertical levels. This work utilized results from the 4 km domain. The modeling domains are shown in Figures 3 and 4. WRF was run straight through (i.e., was not re-initialized at all) using an iterative technique developed at the EPA and described in Appel et al. (2014). Observational and analysis nudging were performed on all domains. Model output was saved hourly for the 36 and 12 km domains, every 20 minutes for the 4 km domain, and every 5 minutes for the 1 km domain. WRF and CMAQ configuration options and inputs are shown in Table 1.

WRF model results were used to drive the CMAQ model offline. The CMAQ model was run with the process analysis tool to output ozone production rate ($P(O_3)$), ozone loss rate ($L(O_3)$), and net ozone production rate (net $P(O_3)$) as well as ozone production efficiency (OPE).

Atmos. Chem. Phys. Discuss., doi:10.5194/acp-2016-215, 2016
Manuscript under review for journal Atmos. Chem. Phys.
Published: 13 May 2016

Atmospheric Chemistry and Physics Discussions

186

187 **3. RESULTS**

188 **3.1 Photochemical O_3 Production Rate, Sensitivity, and Diurnal Variations**

189 Figure 5 shows the net ozone production rate, net $P(O_3)$, calculated using the box model
190 results along the P-3B flight track for all flight days during the Houston deployment. There are
191 several $P(O_3)$ hotspots over the Houston Ship Channel located to the east/southeast of downtown
192 Houston as well as downwind, over Galveston Bay. This is expected because of large emissions
193 of NO_x and VOCs from the Houston Ship Channel, where the highest $P(O_3)$ was observed – up
194 to ~140 ppbv hr^{-1}. $P(O_3)$ values up to ~80-90 ppbv hr^{-1} were observed over Galveston Bay,
195 mainly on September 25, 2013, consistent with high ozone levels observed cross the Houston
196 area on that day.

197 Figure 6 shows the indicator L_N/Q of ozone production sensitivity along the P-3B flight
198 track for all flight days during the Houston deployment. $P(O_3)$ was mainly VOC-sensitive over
199 the Houston Ship Channel and its surrounding urban areas due to large NO_x emissions. Over
200 areas away from the center of the city with relatively low NO_x emissions, $P(O_3)$ was usually
201 NOx-sensitive. Vertical profiles of $P(O_3)$, $L(O_3)$, and net ozone production calculated using the
202 box model results (Figure 7) show that:
203 (1) $RO_2 + NO$ makes about the same amount of O_3 as $HO_2 + NO$ in the model;
204 (2) O_3 photolysis followed by $O(^1D)+H_2O$ is a dominant process for the photochemical ozone
205 loss;
206 (3) the maximum net $P(O_3)$ appeared near the surface below 1 km.

207 In the diurnal variations of $P(O_3)$, a broad peak in the morning with significant $P(O_3)$ in
208 the afternoon was obtained on ten flight days during DISCOVER-AQ in Houston (Figure 8).
209 High $P(O_3)$ mainly occurred with $L_N/Q > 0.5$ (i.e., in the VOC sensitive regime). The diurnal
210 variation of L_N/Q indicates that $P(O_3)$ was mainly VOC sensitive in the early morning and then
211 transitioned towards the NO_x sensitive regime later in the day (Figure 9). High $P(O_3)$ in the
212 morning was mainly associated with VOC sensitivity due to high NO_x levels in the morning
213 (points in the red circle in Figure 9). Although $P(O_3)$ was mainly NO_x sensitive in the afternoon
214 between 12:00 and 17:00 Central Standard Time, CST (UTC-5), there were also periods and
215 locations when $P(O_3)$ was VOC sensitive, e.g., the points above the red line in Figure 8.

Atmos. Chem. Phys. Discuss., doi:10.5194/acp-2016-215, 2016
Manuscript under review for journal Atmos. Chem. Phys.
Published: 13 May 2016

Atmospheric Chemistry and Physics Discussions

Diurnal variations of ozone production rate at eight individual locations where the P-3B conducted vertical spirals show that the ozone production is greater than 10 ppb hr^{-1} on average at locations with high NO_x and VOC emissions such as Deer Park, Moody Tower and Channelview, while at locations away from the urban center with lower emissions such as Galveston, Smith Point, and Conroe, the ozone production usually averaged less than 10 ppb hr^{-1} (Figure 10). The dependence of $P(O_3)$ on the NO mixing ratio ([NO]) shows that when [NO] is less than ~1 ppbv, ozone production increases as the [NO] increases, i.e., $P(O_3)$ is in NOx sensitive regime. When the NO mixing ratio is greater than ~1 ppbv, ozone production levels off, i.e., $P(O_3)$ is in a NOx saturated regime (Figure 11). It was also found that at a given NO mixing ratio, a higher production rate of HO_x results in a higher ozone production rate. Diurnal variations of the indicator of ozone production sensitivity to NO_x and VOCs, L_N/Q, at eight individual locations where the P-3B conducted vertical spirals show that (1) at Deer Park, $P(O_3)$ was mostly VOC sensitive for the entire day; (2) at Moody Tower and Channelview, $P(O_3)$ was VOC sensitive or in the transition regime; and (3) at Smith Point and Conroe, $P(O_3)$ is mostly NOx sensitive for the entire day; and Galveston, West Houston, and Manvel Croix were VOC sensitive only in the early morning (Figure 12).

3.2 Ozone Production Efficiency

Ozone production efficiency (OPE) is defined as the number of molecules of oxidant Ox (= O_3 + NO_2) produced photochemically when a molecule of NO_x (= NO + NO_2) is oxidized. It conveys information about the conditions under which O_3 is formed and is an important parameter to consider when evaluating impacts from NO_x emission sources [Kleinman et al., 2002]. The OPE can be deduced from atmospheric observations as the slope of a graph of O_x concentration versus the concentration of NO_x oxidation products. The latter quantity is denoted as NO_z and is commonly measured as the difference between NO_y (sum of all odd-nitrogen compounds) and NO_x, i.e. $NO_z = NO_y - NO_x$.

Figure 13 shows the photochemical oxidant O_x as a function of NO_z during DISCOVER-AQ in Houston in 2013. The two data sets plotted here were collected on September 25 and 26, when high ambient ozone concentrations were observed, and for the data collected during all other flights. Note that the slopes obtained from these two data sets are essentially the same and an average OPE of ~8 is derived from the observations, meaning that 8 molecules of ozone were

Atmos. Chem. Phys. Discuss., doi:10.5194/acp-2016-215, 2016
Manuscript under review for journal Atmos. Chem. Phys.
Published: 13 May 2016

produced when one molecule of NO_x was consumed. Even though higher ozone concentrations were observed on September 25 and 26, the OPE on these two days are not different from those in other flights, indicating the ozone event on these two days was not caused by a higher OPE, but mainly, by higher concentrations of ozone precursors (and thus higher ozone production rates) and background ozone as indicated by the intercepts in the regression of the two data sets in Figure 13**.** The high ozone observed on those days could also be due to slower ventilation and different meteorological conditions such as a lower boundary layer height, northerly transport, stagnant conditions from the high-pressure system, and the bay and gulf breezes.

The OPE value during DISCOVER-AQ in Houston in 2013 is greater than the average OPE value (5.9±1.2) obtained during the Texas Air Quality Study in 2006 (TexAQS2006) [Neuman et al., 2009]. One possible reason for this increased OPE is the continuous reduction in NO_x emissions in Houston between 2006 and 2013 pushed NO_x levels closer to 1 ppbv in 2013, thus OPE increased since OPE increases as NO_x decreases when the NO_x level is greater than ~1 ppbv (Figure 14). This OPE value is about a factor of 1.5 to 2 higher than the OPEs obtained in the DISCOVER-AQ 2011 study in Maryland ranging from 4 to 5.5 (Ren, X., unpublished data), due to higher photochemical reactivity in Houston.

When calculating ozone production efficiency, it is important to know whether there is substantial loss of nitric acid (HNO_3), because it can affect the OPE by reducing the NO_z [Trainer et al., 1993; 2000; Neuman et al., 2009] and thus bias the OPE high. The derived OPE in Figure 13 is only valid when there is minimum loss of NO_z (especially HNO_3) from the source region to the point of observations. Neuman et al. [2009] found that $\Delta CO/\Delta NOy$, i.e., the slope in a CO versus NO_y plot, is an indicator for distinguishing plumes with efficient O_3 formation from plumes with similarly high O_3 to NO_x oxidation products correlation slopes caused by variable mixing of aged polluted air depleted in HNO_3. A typical $\Delta CO/\Delta NO_y$ ranges from ~40 in background air to ~4-7 in fresh emission plumes in Houston [Neuman et al., 2009]. The $\Delta CO/\Delta NO_y$ was examined at different times of the day on September 25 and 26. The results indicate that the $\Delta CO/\Delta NO_y$ was about 6.2 (Figure 15a) throughout the day with variation between 6.0 and 7.0 (Figure 15). This demonstrates that the observed O_3 formation was from fresh plumes and was not caused by variable mixing of aged polluted air depleted in HNO_3.

Using both the box model and CMAQ model results, OPE can also be calculated according to its definition, i.e., the net ozone formation rate divided by of the formation rate of

Atmos. Chem. Phys. Discuss., doi:10.5194/acp-2016-215, 2016
Manuscript under review for journal Atmos. Chem. Phys.
Published: 13 May 2016

278 NO_z. Net $P(O_3)$ was calculated using Eq. (1), while the NO_z formation rate is the sum of HNO_3
279 and organic nitrate formation rates. The agreement between the box model-derived and the
280 CMAQ-derived OPEs is very good, with the mean OPEs of 14.8±7.4 in the box model and
281 16.6±8.1 in the CMAQ model. The dependence of OPE on NO_x is also similar for both the box
282 and CMAQ models (Figure 14). On average, the maximum of OPE appears at a NO_x level
283 around 1 ppbv. With the NO_x level below 1 ppbv, OPE increases as the NO_x level increases,
284 while with the NO_x level above 1 ppbv, OPE decreases as the NO_x level increases (Figure 14).
285 The OPE values calculated using the CMAQ and box model are greater than the values
286 derived from the observations using the slope in the scatter plot of Ox versus NO_z in Figure 13.
287 This is expected because in the calculation of OPE using the box and CMAQ model results, a
288 few ozone loss processes such as ozone dry deposition and horizontal/vertical dispersion were
289 not considered. This could result in higher calculated ozone production rates using the model
290 results.
291 Spatial variations of OPE demonstrate that except for a few hotspots over Downtown
292 Houston and the Houston Ship Channel, most large OPEs appear away from the urban center,
293 e.g., the northwest and southeast of the area, while in areas with high NO_x emissions close to the
294 urban center lower OPEs were generally observed (Figure 16). This is again consistent with the
295 results in Figure 14 that the maximum of OPE appears at a NO_x level around 1 ppbv.
296
297 **4. Discussion and Conclusions**
298 On average, ozone production $P(O_3)$, was about 20-30 ppbv hr^{-1} in the morning and 5-10
299 ppbv hr^{-1} in the afternoon during DISCOVER-AQ in Houston in 2013. The diurnal variation of
300 $P(O_3)$ shows a broad peak in the morning with significant $P(O_3)$ in the afternoon obtained on ten
301 flight days in September 2013. High $P(O_3)$ mainly occurred with L_N/Q greater than 0.5, i.e., in
302 the VOC sensitive regime. Since $P(O_3)$ depends on NO_x levels and radical production rate, it
303 increases as [NO] increases up to ~1 ppbv and then levels off with further increases of [NO]. At
304 a given [NO], a higher production rate of HO_x results in a higher ozone production rate. This has
305 implications for the NO_x control strategies in order to achieve the ozone control goal.
306 The DISCOVER-AQ campaign in Houston is unique because of its large spatial coverage
307 and thus spatial variations of ozone production and its sensitivity to NOx and VOCs. Diurnal
308 variations of $P(O_3)$ at eight individual locations where the P-3B conducted vertical spirals show

Atmos. Chem. Phys. Discuss., doi:10.5194/acp-2016-215, 2016
Manuscript under review for journal Atmos. Chem. Phys.
Published: 13 May 2016

that the $P(O_3)$ is on average more than 10 ppbv hr^{-1} at locations with high NO_x and VOC emissions, such as Deer Park, Moody Tower, and Channelview, while at locations away from the urban center with lower emissions of ozone precursors such as Galveston, Smith Point, and Conroe, the ozone production rate is usually less than 10 ppbv hr^{-1} on average. Hotspots of $P(O_3)$ were observed over Downtown Houston and Houston Ship Channel due to significant emissions in these areas.

Ozone production tended more towards VOC sensitive in the morning with high $P(O_3)$ and in general, NO_x sensitive in the afternoon with some exceptions. It was found that during some afternoon time periods and locations, $P(O_3)$ was VOC sensitive. The diurnal variation of L_N/Q indicates that $P(O_3)$ was mainly VOC sensitive in the early morning and then transited towards the NO_x sensitive regime later in the day. High $P(O_3)$ in the morning was mainly associated with VOC sensitivity due to high NO_x levels in the morning. Specifically, Deer Park was mostly VOC sensitive for the entire day, Moody Tower and Channelview were VOC sensitive or in the transition regime, and Smith Point and Conroe were mostly NO_x sensitive for the entire day.

Based on the measurements on the P-3B, ozone production efficiency (OPE) was about 8 during DISCOVER-AQ 2013 in Houston. This OPE value is greater than the average OPE value (5.9±1.2) obtained during the Texas Air Quality Study in 2006 (TexAQS2006), likely due to the reduction in NO_x emissions in Houston between 2006 and 2013 that pushed NO_x levels closer to 1 ppbv in 2013 from higher NOx levels in previous years. This OPE value is about a factor of 1.5 to 2 higher than the OPE obtained in the DISCOVER-AQ 2011 study in Maryland due to higher photochemical reactivity in Houston.

The results from this work strengthen our understanding of O_3 production; they indicate that controlling NO_x emissions will provide air quality benefits over the greater Houston metropolitan area in the long run, but in selected areas controlling VOC emissions will also be beneficial.

Acknowledgements

The authors acknowledge the entire DISCOVER-AQ science team for the use of the P-3B measurement data in this work as well as Winston Luke and Paul Kelley at NOAA Air Resources Laboratory for helpful discussion. This work was funded by the Texas Commission

on Environmental Quality (TCEQ) through the Air Quality Research Program (AQRP) at University of Texas Austin (Contract #14-020). The contents, findings, opinions, and conclusions are the work of the authors and do not necessarily represent the findings, opinions, or conclusions of the TCEQ or AQRP. AQAST supported RRD.

References

Appel, K.W., Gilliam, R.C., Pleim, J.E., Pouliot, G.A., Wong, D.C., Hogrefe, C., Roselle, S.J., and Mathur, R.: Improvements to the WRF-CMAQ modeling system for fine-scale air quality simulations, EM, 16-21 2014.

Atkinson, R., et al.: Evaluated kinetic and photochemical data for atmospheric chemistry Volume I - gas phase reactions of Ox, HOx, NOx and SOx species, Atmos. Chem. Phys., 4, 1461-1738, 2004.

Atkinson, R., et al.: Evaluated kinetic and photochemical data for atmospheric chemistry Volume II - gas phase reactions of organic species, Atmos. Chem. Phys., 6, 3625-4055, 2006.

Atkinson, R., et al.: Evaluated kinetic and photochemical data for atmospheric chemistry Volume III - gas phase reactions of inorganic halogens, Atmos. Chem. Phys., 7, 981-1191, 2007.

Atkinson, R., et al., Evaluated kinetic and photochemical data for atmospheric chemistry Volume IV - gas phase reactions of organic halogen species, *Atmos. Chem. Phys.*, 8, 4141-4496, 2008.

Canty, T. P., L. Hembeck, T. P. Vinciguerra, D. C. Anderson, D. L. Goldberg, S. F. Carpenter, D. J. Allen, C. P. Loughner, R. J. Salawitch, and R. R. Dickerson (2015), Ozone and NOx chemistry in the eastern US: evaluation of CMAQ/CB05 with satellite (OMI) data, *Atmospheric Chemistry and Physics*, *15*(19), 10965-10982, doi:10.5194/acp-15-10965-2015.

Chen, S., Ren, X., Mao J., Chen, Z., Brune, W. H., Lefer, B., Rappenglück, B., Flynn J., Olson, J., Crawford, J. H.: A comparison of chemical mechanisms based on TRAMP–2006 field data, Atmos. Environ., 44(33), 4116-4125, 2010.

DISCOVER-AQ whitepaper, http://discover-aq.larc.nasa.gov/pdf/DISCOVER-AQ_science.pdf.

Finlayson-Pitts, B. J., and Pitts, J.: Chemistry of the upper and lower atmosphere: Theory, experiments and applications, Academic Press, San Diego, California, p.264-276, 2000.

Goldberg, D. L., Vinciguerra, T. P., Anderson, D. C., Hembeck, L., Canty, T. P., Salawitch, R. J.,

371 and Dickerson, R. R. CAMx Ozone Source Attribution in the Eastern United States using
372 Guidance from Observations during DISCOVER-AQ Maryland, *Geophysical Research*
373 *Letters*, doi: 10.1002/2015GL067332, 2016.,
374 Jacob, D. J., Introduction to Atmospheric Chemistry, Princeton University Press, New Jersey,
375 1999.
376 Kleinman, L. I., Daum, P. H., Lee, Y.-N, Nunnermacker, L. J., Springston, S. R., Weinstein-
377 Lloyd J., and Rudolph, J.: Sensitivity of ozone production rate to ozone precursors. Geophys.
378 Res. Lett., 28, 2903–2906 , doi: 10.1029/2000GL012597, 2001.
379 Kleinman, L. I., Daum, P. H., Lee, Y.-N., Nunnermacker, L. J., Springston, S. R., Weinstein-
380 Lloyd, J., and Rudolph, J.: Ozone production efficiency in an urban area, J. Geophys. Res.,
381 107 (D23), 4733, doi:10.1029/2002JD002529, 2002.
382 Kleinman, L. I., Daum, P. H., Lee, Y.-N., Nunnermacker, L. J., Springston, S. R., Weinstein-
383 Lloyd, J., and Rudolph, J.: A comparative study of ozone production in five U.S.
384 metropolitan areas, J. Geophys. Res., 110, D02301, doi:10.1029/2004JD005096, 2005a.
385 Kleinman, L. I.: The dependence of tropospheric ozone production rate on ozone precursors,
386 Atmos. Environ., 39(3), 575–586, doi:10.1016/j.atmosenv.2004.08.047, 2005b.
387 Lei, W., Zhang, R., Tie, X., and Hess, P.: Chemical characterization of ozone formation in the
388 Houston-Galveston area: A chemical transport model study, J. Geophys. Res., 109, D12301,
389 doi:10.1029/2003JD004219, 2004.
390 Li, G., Zhang, R., Fan, J., and Tie, X.: Impacts of biogenic emissions on photochemical ozone
391 production in Houston, Texas, J. Geophys. Res., 112, D10309, doi:10.1029/2006JD007924,
392 2007.
393 Mallet, V. and Sportisse, B.: A comprehensive study of ozone sensitivity with respect to
394 emissions over Europe with a chemistry-transport model, J. Geophys. Res., 110, D22302,
395 doi:10.1029/2005JD006234, 2005.
396 Mao, J., Ren, X., Chen, S., Brune, W. H., Chen, Z., Martinez, M., Harder, H., Lefer, B.,
397 Rappenglück, B., Flynn, J., and Leuchner, M.: Atmospheric oxidation capacity in the
398 summer of Houston 2006: Comparison with summer measurements in other metropolitan
399 studies, Atmos. Environ., 44(33), 4107-4115, 2010
400 Molina, M. J., and Molina, L. T.: Megacities and atmospheric pollution, J. Air Waste Manage.,
401 54, 644–680, 2004.

Neuman, J. A., et al.: Relationship between photochemical ozone production and NOx oxidation in Houston, Texas, J. Geophys. Res., 114, D00F08, doi:10.1029/2008JD011688, 2009.

Ren, X., van Duin, D., Cazorla, M., Chen, S., Mao, J., Zhang, L., Brune, W. H., Flynn, J. H., Grossberg, N., Lefer, B. L., Rappenglück, B., Wong, K. W., Tsai, C., Stutz, J., Dibb, J. E., Jobson, B. T., Luke, W. T., and Kelley, P.: Atmospheric oxidation chemistry and ozone production: Results from SHARP 2009 in Houston, Texas, J. Geophys. Res., 118, 5770–5780, 2013.

Sander, S. P., Abbatt, J., Barker, J. R., Burkholder, J. B., Friedl, R. R., Golden, D. M., Huie, R. E., Kolb, C. E., Kurylo, M. J., Moortgat, G. K., Orkin V. L., and Wine, P. H.: Chemical Kinetics and Photochemical Data for Use in Atmospheric Studies, Evaluation No. 17, JPL Publication 10-6, Jet Propulsion Laboratory, Pasadena, 2011.

Sillman, S.: The use of NO_y, H_2O_2, and HNO_3 as indicators for O_3-NO_x-hydrocarbon sensitivity in urban locations, J. Geophys. Res., 100, 14,175–14,188, 1995.

Sillman, S., Vautard, R., Menut, L., and Kley, D.: O_3-NO_x-VOC sensitivity and NO_x-VOC indicators in Paris: Results from models and Atmospheric Pollution Over the Paris Area (ESQUIF) measurements, J. Geophys. Res., 108(D17), 8563, doi:10.1029/2002JD001561, 2003.

Tang, X., Wang, Z., Zhu, J., Gbaguidi, A. E., Wu, Q., Li, J., and Zhu, T., Sensitivity of ozone to precursor emissions in urban Beijing with a Monte Carlo scheme. Atmos. Environ., 44, 3833-3842, 2010.

Trainer, M., et al.: Correlation of ozone with NOy in photochemically aged air, J. Geophys. Res., 98, 2917 – 2925, doi:10.1029/ 92JD01910, 1993.

Trainer, M., Parrish, D. D., Goldan, P. D., Roberts, J., and Fehsenfeld, F. C.: Review of observation-based analysis of the regional factors influencing ozone concentrations, Atmos. Environ., 34, 2045 – 2061, doi:10.1016/S1352-2310(99)00459-8, 2000.

Xue, L. K., Wang, T., Gao, J., Ding, A. J., Zhou, X. H., Blake, D. R., Wang, X. F., Saunders, S. M., Fan, S. J., Zuo, H. C., Zhang, Q. Z., and Wang, W. X.: Ozone production in four major cities of China: sensitivity to ozone precursors and heterogeneous processes, Atmos. Chem. Phys. Discuss., 13, 27,243–27,285, doi:10.5194/acpd-13-27243-2013, 2013.

Yarwood, G., Rao, S., Yocke, M., and Whitten, G. Z.: Updates to the Carbon Bond Mechanism: CB05, Final Report to the US EPA (RT-0400675),(http://www.camx.com/publ/

Atmos. Chem. Phys. Discuss., doi:10.5194/acp-2016-215, 2016
Manuscript under review for journal Atmos. Chem. Phys.
Published: 13 May 2016

433 pdfs/CB05_Final_Report_120805.pdf), 2005.

Atmos. Chem. Phys. Discuss., doi:10.5194/acp-2016-215, 2016
Manuscript under review for journal Atmos. Chem. Phys.
Published: 13 May 2016

Atmospheric Chemistry and Physics Discussions

434 **Table** 1. WRF and CMAQ model options that were used in both the original and improved
435 modeling scenarios.

Weather Research and Forecasting (WRF) Version 3.6.1 Model Options	
Radiation	Long Wave: Rapid Radiative Transfer Model (RRTM) Short Wave: Goddard
Surface Layer	Pleim-Xiu
Land Surface Model	Pleim-Xiu
Boundary Layer	Asymmetric Convective Model (ACM2)
Cumulus	Kain-Fritsch
Microphysics	WRF Single-Moment 6 (WSM-6)
Nudging	Observational and analysis nudging
Damping	Vertical velocity and gravity waves damped at top of modeling domain
SSTs	Multi-scale Ultra-high Resolution (MUR) SST analysis (~1 km resolution)
Meteorological Initial and Boundary Conditions and Analysis Nudging Inputs	NAM 12 km
Observational Nudging Inputs	NCEP ADP Global Surface and Upper Air Observational Weather Data
CMAQ Version 5.0.2 Model Options	
Chemical Mechanism	Carbon Bond (CB05)
Aerosol Module	Aerosols with aqueous extensions version 5 (AE5)
Dry deposition	M3DRY
Vertical diffusion	Asymmetric Convective Model 2 (ACM2)
Emissions	2012 TCEQ anthropogenic emissions Biogenic Emission Inventory System (BEIS) calculated within CMAQ
Chemical Initial and Boundary Conditions	Model for OZone and Related chemical Tracers (MOZART) Chemical Transport Model (CTM)

436
437
438
439
440
441
442
443
444

Atmos. Chem. Phys. Discuss., doi:10.5194/acp-2016-215, 2016
Manuscript under review for journal Atmos. Chem. Phys.
Published: 13 May 2016

Atmospheric Chemistry and Physics Discussions

445 **Figures:**

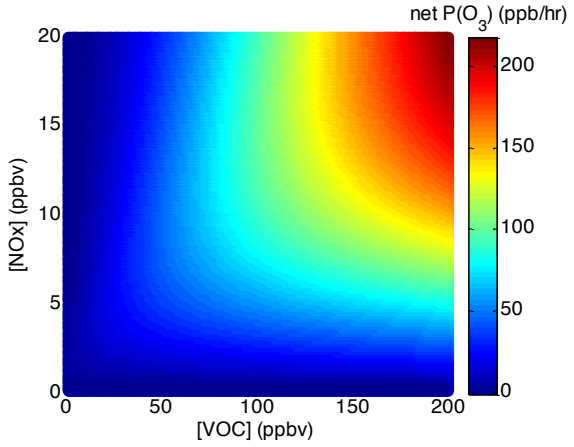

446

447 **Figure 1.** Ozone production empirical kinetic modeling approach (EKMA) diagram using a box
448 model results with NOx levels varying from 0-20 ppbv and VOC levels from 0-200 ppbv while
449 the mean concentrations of other species and the speciation of NOx and VOCs observed during
450 DISCOVER-AQ in Houston in 2013 were used to constrain the box model. This diagram clearly
451 shows the sensitivity of ozone production to NO_x and VOCs in Houston.

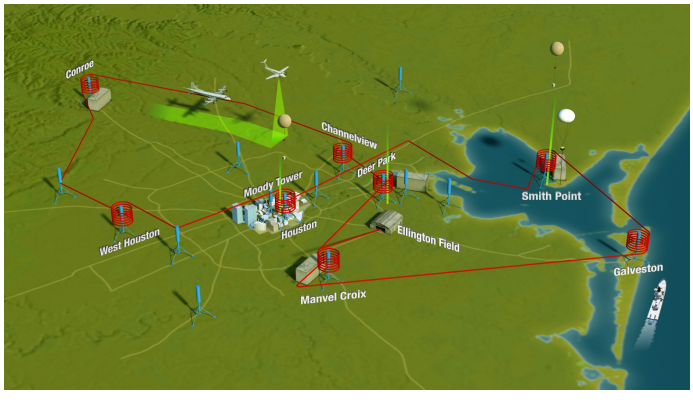

452

453 **Figure 2.** DISCOVER-AQ ground and spiral sites during the September 2013 Houston
454 campaign (http://discover-aq.larc.nasa.gov).

455

Atmos. Chem. Phys. Discuss., doi:10.5194/acp-2016-215, 2016
Manuscript under review for journal Atmos. Chem. Phys.
Published: 13 May 2016

Atmospheric Chemistry and Physics Discussions

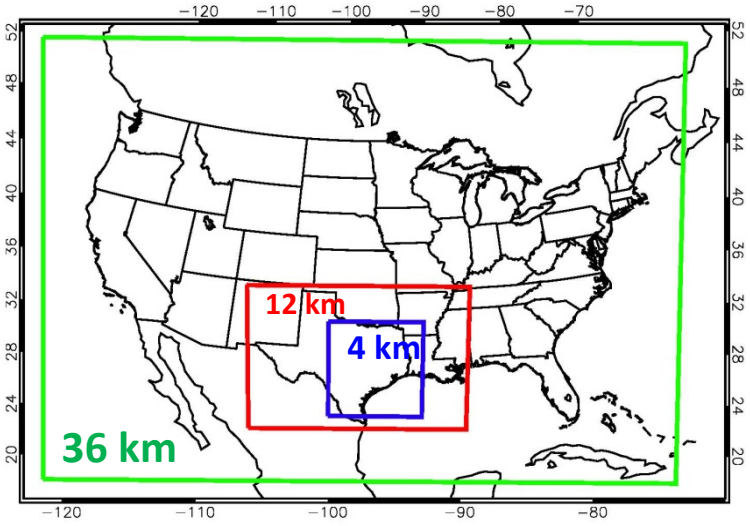

456

457 **Figure 3.** 36, 12, and 4 km CMAQ modeling domains

458

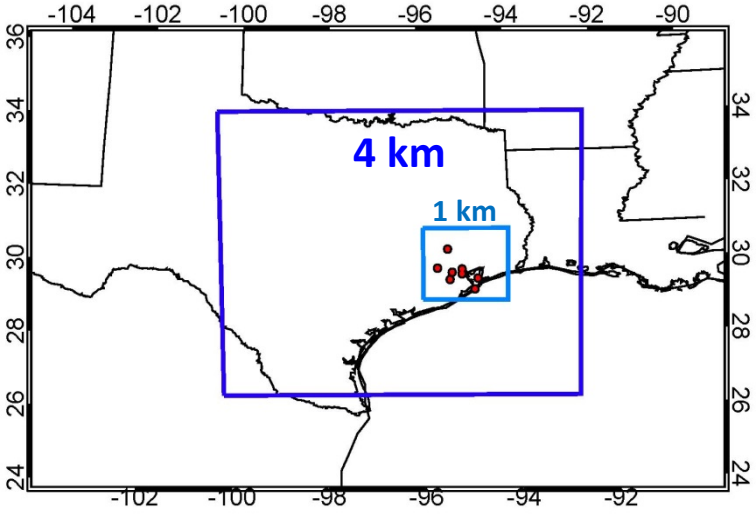

459

460 **Figure 4.** 4 and 1 km CMAQ modeling domains. The red dots show the NASA P-3B aircraft
461 spiral locations.

462

Atmos. Chem. Phys. Discuss., doi:10.5194/acp-2016-215, 2016
Manuscript under review for journal Atmos. Chem. Phys.
Published: 13 May 2016

Atmospheric Chemistry and Physics Discussions

463

464

465

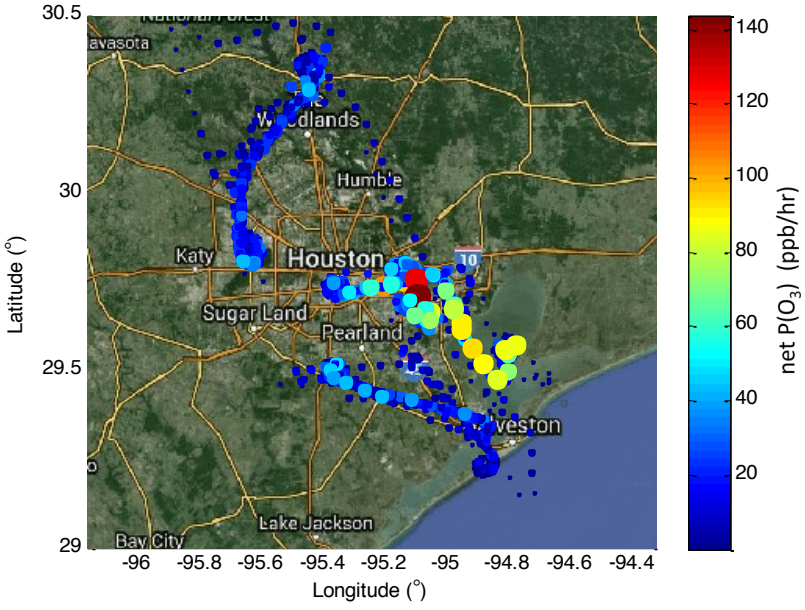

466

467 **Figure 5.** Net ozone production rate, net $P(O_3)$ calculated using the box model results along the
468 P-3B flight track during DISCOVER-AQ in Houston in 2013. The size of dots is proportional to
469 $P(O_3)$.

Atmos. Chem. Phys. Discuss., doi:10.5194/acp-2016-215, 2016
Manuscript under review for journal Atmos. Chem. Phys.
Published: 13 May 2016

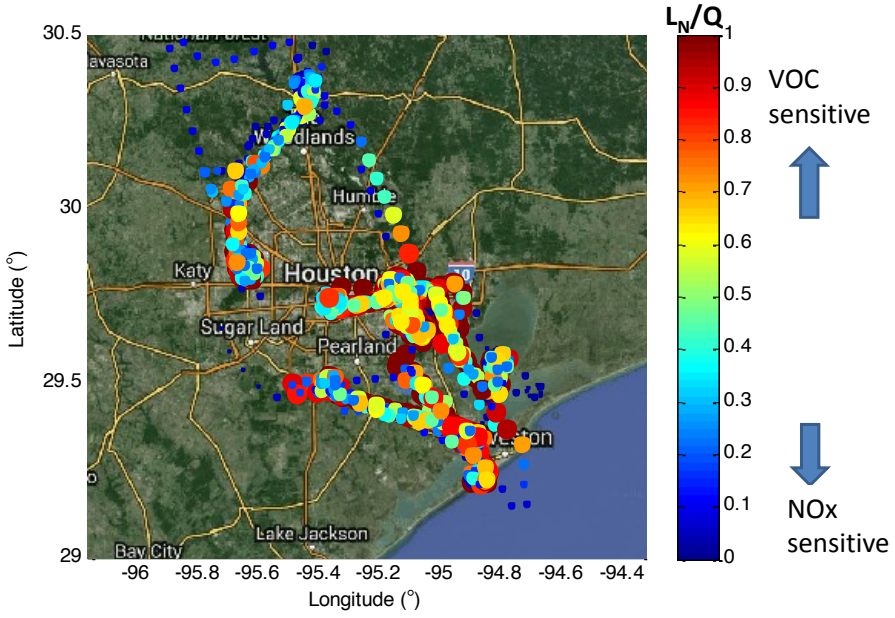

470

471 **Figure 6.** Ozone production sensitivity indicator, L_N/Q, along the P-3B flight track during
472 DISCOVER-AQ in Houston in 2013. $P(O_3)$ is VOC-sensitive when $L_N/Q > 0.5$, and NOx-
473 sensitive when $L_N/Q < 0.5$.

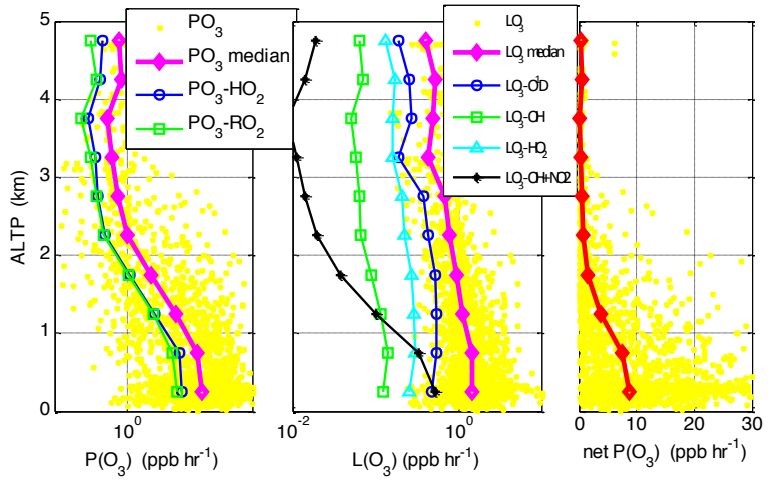

474

475 **Figure 7.** Vertical profiles of ozone production rate (left), ozone loss rate (middle), and net
476 ozone production rate (right) during DISCOVER-AQ in Houston in 2013.

Atmos. Chem. Phys. Discuss., doi:10.5194/acp-2016-215, 2016
Manuscript under review for journal Atmos. Chem. Phys.
Published: 13 May 2016

Atmospheric Chemistry and Physics Discussions

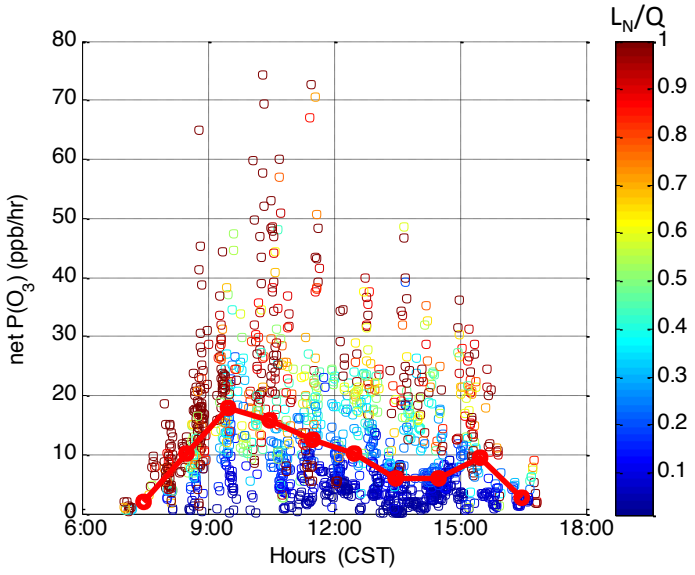

Figure 8. Diurnal variation of ozone production rate colored with the indicator L_N/Q on ten flight days during DISCOVER-AQ in Houston in 2013. The solid red circles represent the median values in hourly bins of $P(O_3)$. Data are limited with the pressure altitude less than 1000 m to represent the lowest layer of the atmosphere.

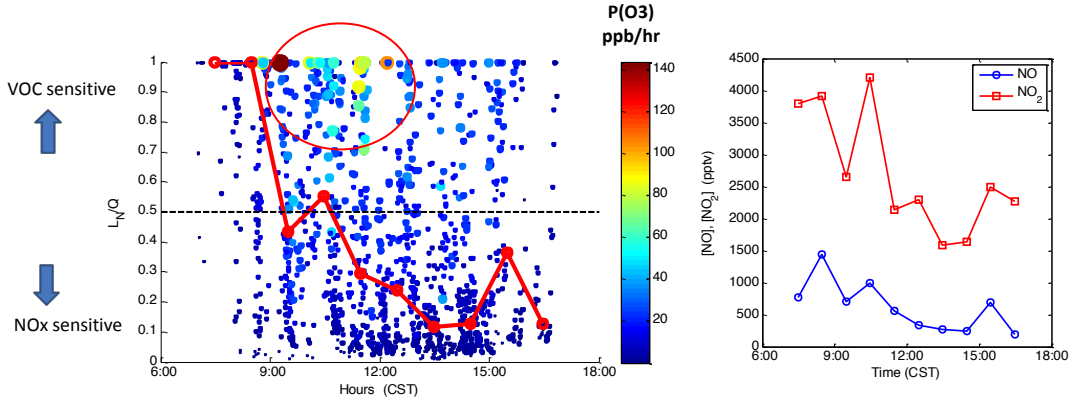

Figure 9. Diurnal variations of the indicator L_N/Q of ozone production rate sensitivity colored with ozone production rate (left) and NO and NO_2 concentrations (right) below 1000 m during DISCOVER-AQ in Houston in 2013. The solid red circles are the median values in hourly bins of L_N/Q.

Atmos. Chem. Phys. Discuss., doi:10.5194/acp-2016-215, 2016
Manuscript under review for journal Atmos. Chem. Phys.
Published: 13 May 2016

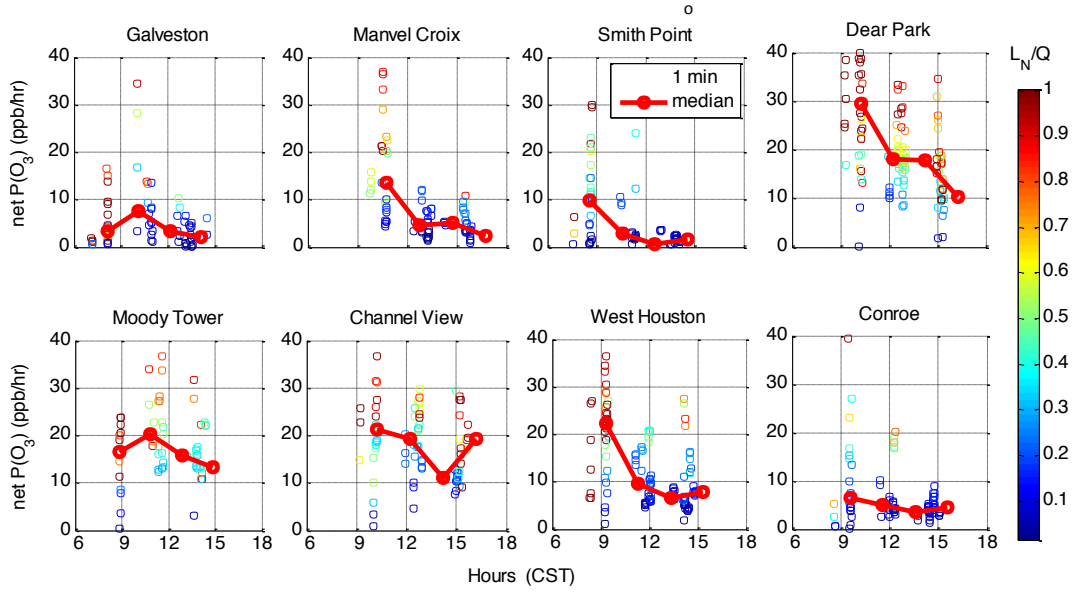

Figure 10. Diurnal variations of ozone production rate at eight individual spiral locations. Individual points are 1-min data colored with L_N/Q and the linked red circles represent the median values in hourly bins of $P(O_3)$. Data are limited with the pressure altitude less than 1000 m to represent the lowest layer of the atmosphere.

Atmos. Chem. Phys. Discuss., doi:10.5194/acp-2016-215, 2016
Manuscript under review for journal Atmos. Chem. Phys.
Published: 13 May 2016

Atmospheric Chemistry and Physics Discussions

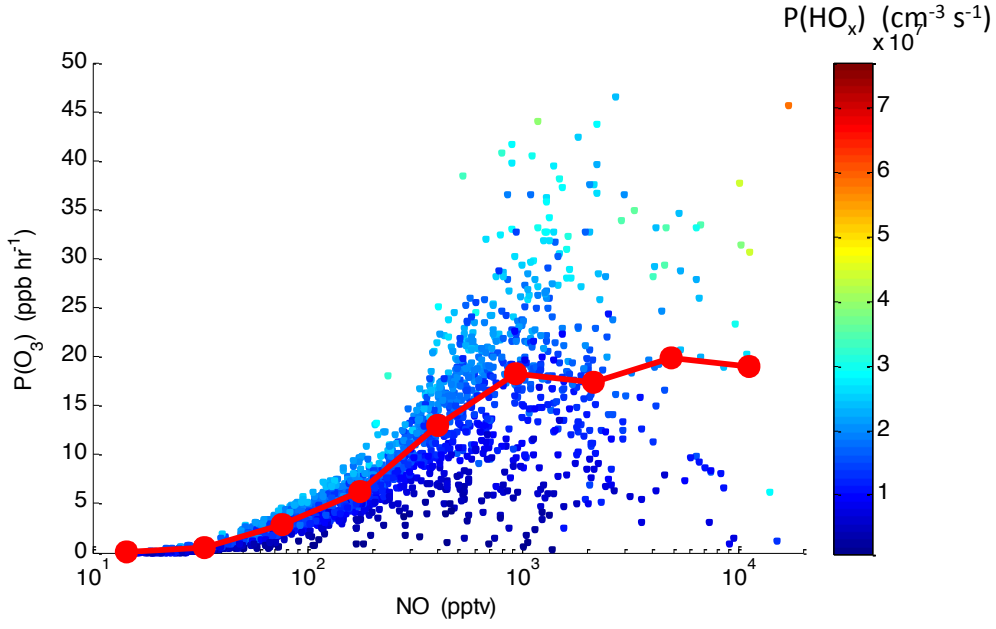

Figure 11. Ozone production as a function of NO mixing ratio. Individual data points are the 1-minute averages and are colored with the production rate of HOx (= OH + HO_2) during DISCOVER-AQ in Houston in 2013. The linked solid red circles represent the median values in [NO] bins. Note a log scale is used for the x-axis.

Atmos. Chem. Phys. Discuss., doi:10.5194/acp-2016-215, 2016
Manuscript under review for journal Atmos. Chem. Phys.
Published: 13 May 2016

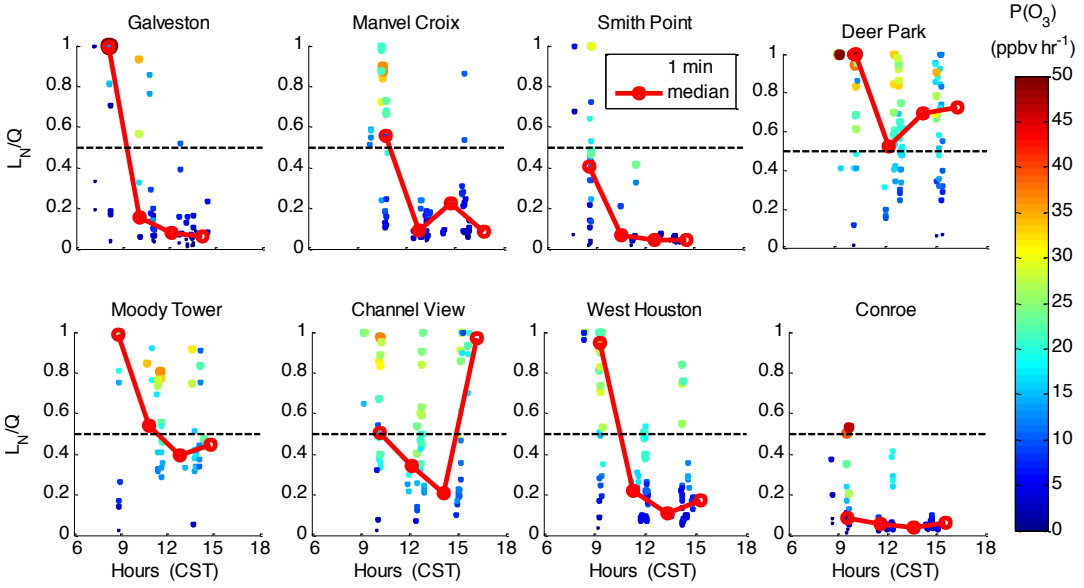

Figure 12. Diurnal variations of the indicator of ozone production sensitivity to NOx and VOCs, L_N/Q, at eight individual spiral locations during DISCOVER-AQ in Houston in 2013. Individual points are 1-min data colored by $P(O_3)$ and the linked red circles represent the median values in hourly bins of $P(O_3)$. Data are limited with the pressure altitude less than 1000 m to represent the lowest layer of the atmosphere.

Atmos. Chem. Phys. Discuss., doi:10.5194/acp-2016-215, 2016
Manuscript under review for journal Atmos. Chem. Phys.
Published: 13 May 2016

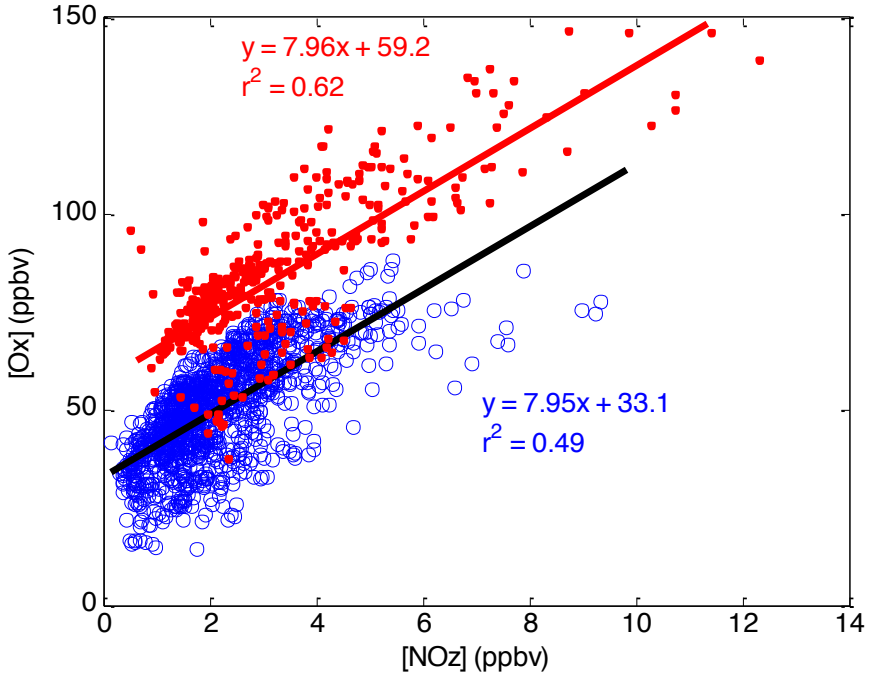

508

509 **Figure 13.** Photochemical oxidant, Ox (=O_3+NO_2) as a function of NOz (=NOy-NOx) during
510 DISCOVER-AQ in Houston in 2013. Red dots are the data collected on September 25 and 26,
511 2013 when high ambient ozone concentrations were observed. Blue circles are the data collected
512 during other flights. Data are limited with the pressure altitude less than 1000 m to represent the
513 lowest layer of the atmosphere.

514

515

516

517

518

Atmos. Chem. Phys. Discuss., doi:10.5194/acp-2016-215, 2016
Manuscript under review for journal Atmos. Chem. Phys.
Published: 13 May 2016

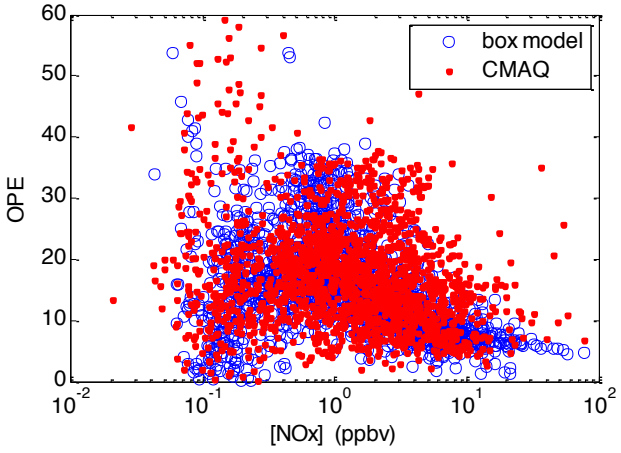

519

520 **Figure 14.** Ozone production efficiency (OPE) versus NOx in the box model (blue circles) and
521 CMAQ model (red dots) results. OPE is calculated according to its definition as the net ozone
522 formation rate divided by of the formation rate of NOz.

523

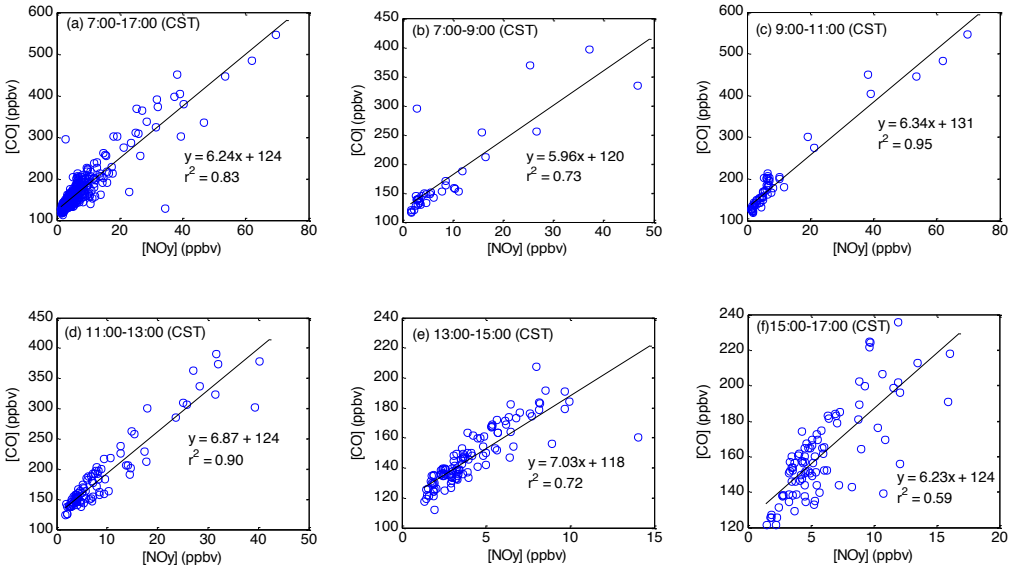

524

525

526 **Figure 15.** CO versus NOy and linear regression on September 25 and 26 at different times of
527 the day: (a) 07:00-17:00 (all data), (b) 07:00-09:00, (c) 09:00-11:00, (d) 11:00-13:00, (e) 13:00-
528 15:00, and (f) 15:00-17:00 (CST).

Atmos. Chem. Phys. Discuss., doi:10.5194/acp-2016-215, 2016
Manuscript under review for journal Atmos. Chem. Phys.
Published: 13 May 2016

Atmospheric Chemistry and Physics Discussions

529

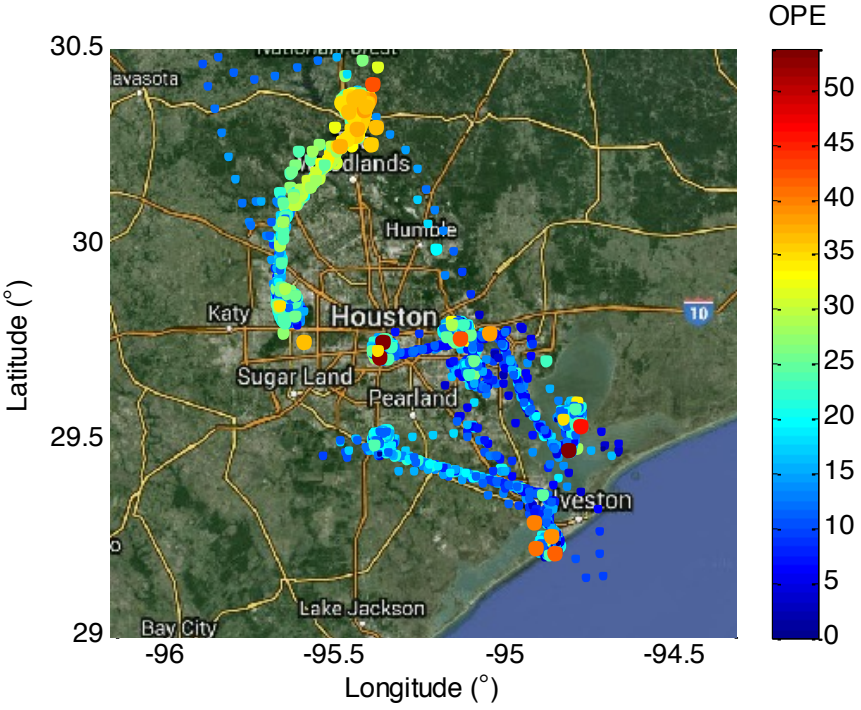

530

531 **Figure 16.** Ozone production efficiency (OPE) along the P-3B flight track during DISCOVER-
532 AQ in Houston in 2013. OPE was calculated using the box model results as the ratio of net ozone
533 formation rate to the formation rate of NOz.

534